Umbilical cord blood-derived Helios-positive regulatory T cells promote angiogenesis in acute lymphoblastic leukemia in mice via CCL22 and the VEGFA-VEGFR2 pathway

XUE LI[1], DONG LI[1,2], QING SHI[1,2], XIAOYANG HUANG[1] and XIULI JU[1,2]

[1]Department of Pediatrics, Qilu Hospital; [2]Stem Cell And Regenerative Medicine Research Center, Shandong University, Jinan, Shandong 250012, P.R. China

Received October 29, 2018; Accepted February 28, 2019

DOI: 10.3892/mmr.2019.10074

Abstract. Regulatory T cells (Tregs) maintain immune homeostasis and modulate tumor-induced neovascularization. However, the mechanisms underlying the role of Tregs in acute lymphoblastic leukemia (ALL) remain to be elucidated. Helios, combined with forkhead box P3, is considered a suitable marker for discriminating functional Tregs. In the present study, a microenvironment was created with a high proportion of Helios$^+$ Tregs in T cell-deficient nude mice to determine the mechanism underlying Tregs expressing Helios in ALL. It was revealed that umbilical cord blood-derived Helios$^+$ Tregs had proliferation and immunosuppression abilities similar to those of normal pediatric Tregs. The accumulation of Helios$^+$ Tregs accelerated leukemogenesis and the infiltration of leukemic cells into the bone marrow. Importantly, a high expression of Helios in Tregs promoted angiogenesis in the bone marrow via the vascular endothelial growth factor (VEGF)A/VEGF receptor 2 (VEGFR2) pathway. Furthermore, the expression of chemokine CC-chemokine ligand 22 (CCL22) in the bone marrow and serum of ALL mice infused with Helios^{high} Treg cells was increased. The results demonstrated that Helios promotes the secretion of chemokine CCL22, which may recruit more Tregs into the bone marrow. Increased Helios$^+$ Treg cells promoted angiogenesis in the bone marrow of ALL mice via the VEGFA/VEGFR2 pathway. Therefore, Helios may be a target to manipulate Treg activity in clinical settings.

Correspondence to: Dr Xiuli Ju, Department of Pediatrics, Qilu Hospital, Shandong University, 107 West Wenhua Road, Jinan, Shandong 250012, P.R. China
E-mail: 2005duola@163.com

Key words: Helios, regulatory T cells, acute lymphoblastic leukemia, angiogenesis, umbilical cord blood, vascular endothelial growth factor, CC-chemokine ligand 22

Introduction

Immunosuppression mediated by regulatory T cells (Tregs) is considered to be a key facilitator of tumor immune evasion (1,2). Marked Treg infiltration into tumors is generally associated with pathogenesis and a poor clinical outcome (3). In addition to the immunosuppressive function of Tregs, emerging evidence suggests a link between angiogenesis and the accumulation of Tregs at tumor sites (4,5).

Previous studies have shown that Tregs contribute to tumor angiogenesis through indirect and direct mechanisms. Tregs can promote angiogenesis indirectly by inhibiting effector cell-derived angiostatic cytokines, including interferon γ (IFN-γ) and C-X-C motif chemokine 10 (CXCL10) (6). Tregs that have been recruited to hypoxic regions can also directly stimulate angiogenesis through the production of vascular endothelial growth factor (VEGF) (4). The association of Treg infiltration with the overexpression of VEGF and increased microvessel density in endometrial and breast cancer has provided clinical clues for a link between Tregs and angiogenesis (6). VEGF promoted the proliferation of Tregs, and VEGF/VEGF receptor (VEGFR) antibodies and inhibitors decreased the number of Tregs in patients with colon cancer and in mouse models (7). Sustained angiogenesis is also critical for leukemogenesis (8). Our previous study demonstrated that the expression of Helios in Tregs was involved in angiogenesis *in vitro* (9).

Helios, a member of the Ikaros family, serves an important role in the regulation of lymphoid cell proliferation and differentiation (10). The findings of previous studies have led to increased interest in Helios, which may serve a critical role in controlling certain aspects of Tregs, including their suppressive function, differentiation and survival (10,11). Our previous study confirmed that the increased proportion of Helios$^+$ Tregs in patients with pediatric acute lymphoblastic leukemia (ALL) serves an important role in the mechanism of oncogenesis, and may be involved in the regulation of bone marrow angiogenesis in ALL (9). However, the mechanism requires further clarification.

The present study aimed to investigate whether the expression of Helios in Tregs influences leukemic angiogenesis *in vivo*, and to examine the mechanism further. To this end, a

number of Helios^{high} Tregs derived from umbilical cord blood (UCB) were infused into nude mice with defective T cell function, and leukemia was established in these mice. The findings suggest the importance of Tregs expressing Helios for angiogenesis in ALL *in vivo*.

Materials and methods

Cell culture. The Nalm-6 human pre-B ALL cell line was provided by Professor Daoxin Ma (Qilu Hospital, Jinan, China). A total of five normal pediatric peripheral blood (PB) samples were obtained from consenting individuals (5 female, ages 5-13) with no history of tumors, antecedent primary hematologic abnormalities or immunodeficiency diseases who underwent orthopedic surgery at the Qilu Hospital (Jinan, China) from May-July 2016. A total of five UCB samples were donated by healthy mothers (ages 23-29) at the Qilu Hospital from May-July 2016. Human umbilical vein endothelial cells (HUVECs) were derived from cryopreserved cells in stem cell and regenerative medicine research center (Shandong University, Jinan, China). The Nalm-6 cells were cultured in complete RPMI-1640 medium (HyClone, GE Healthcare Life Sciences, Logan, UT, USA) containing 10% fetal bovine serum (FBS; Gibco; Thermo Fisher Scientific, Inc., Waltham, MA, USA). The HUVECs were cultured in M199 medium (Gibco; Thermo Fisher Scientific, Inc.) containing 15% FBS and 40 ng/ml fibroblast growth factor (PeproTech, Inc., Rocky Hill, NJ, USA). Monocytes from the UCB or PB were isolated from the samples and cultured in complete RPMI-1640 medium. On day 1, 200 U/ml human recombinant interleukin-2 (rIL-2) (PeproTech, Inc.), 2.5 ng/ml transforming growth factor (TGF)-β (eBioscience; Thermo Fisher Scientific, Inc.), 0.5 μg/ml anti-CD3e (OKT3; eBioscience; Thermo Fisher Scientific, Inc.) and 1 μg/ml anti-CD28 (CD28.2; eBioscience; Thermo Fisher Scientific, Inc.) were added to the medium. In accordance with routine culturing, the cells were passaged every 3 days with the addition of 100 U/ml rIL-2. During the culture period, $CD4^+CD25^+$ Tregs and $CD4^+CD25^-$ T helper (Th) cells were isolated using a $CD4^+CD25^+$ Treg Isolation kit (Miltenyi Biotec GmbH, Bergisch Gladbach, Germany). The purity of the Th and Treg cell populations was >90%, as determined by flow cytometry using a Guava easyCyte 8HT flow cytometer (EMD Millipore, Billerica, MA, USA). The cells were counted using a hemocytometer on days 0, 7, 14, 21 and 28 of the culture period. All cells were cultured at 37˚C under a 5% CO_2 atmosphere. All study participants, including direct participants, blood donors and parent/guardians of child participants, provided written informed consent. The study was approved by the Research Ethics Committee of Qilu Hospital.

Expression of Helios in UCB Tregs. To confirm the role of Helios in Tregs, the expression of Helios was reduced in Treg cells on day 14 of culture. A lentiviral vector was used to silence the expression of Helios in the UCB-derived Tregs on day 14 of the culture period. The lentiviral vectors, GV248-enhanced green fluorescent protein (EGFP) short hairpin (sh) RNA-Helios and GV248-EGFP, were developed by Shanghai GeneChem Co., Ltd. (Shanghai, China; Fig. S1A). The Helios sequence was obtained from GeneBank (accession no. NM_016260). According to the RNAi sequence design principle, multiple RNAi target sequences were designed, and the optimal kinetic parameter target was selected to enter the subsequent experimental procedure. The Helios-targeting shRNA sequences (RNAi-sense 5'-CCGGGGAAGATTGTAAGGAACAAC TCGAGTTGTTCCTTACAATCTTCCTTTTTG-3'; RNAi-antisense, 5'-AATTCAAAAAGGAAGATTGTAAGG AACAACTCGAGTTGTTCCTTACAATCTTCC-3') were designed. These were inserted between the AgeI and EcoRI sites in the GV248 vector (Shanghai GeneChem Co., Ltd.) by homologous recombination using the T4 DNA ligase enzyme.

Cells in the logarithmic growth phase were digested with trypsin 24 h prior to being transfected. The cells were re-suspended at $5.0x10^6$ cells/15 ml in Dulbecco's modified Eagle's medium containing 10% FBS, and maintained at 37˚C in an atmosphere of 5% CO_2 for 24 h until the cells were 70-80% confluent. The cell culture medium was replaced with serum-free medium 2 h prior to transfection. DNA was extracted using the Plasmid Maxi kit (Qiagen China Co., Ltd., Shanghai, China), according to the manufacturer's instructions. A solution containing the prepared DNA (20 μg pGV-shRNA vector, 15 μg pHelper vector 1.0 and 10 μg pHelper vector 2.0) was added to a sterile centrifuge tube, and the final volume was brought to 1 ml. The solution was incubated at room temperature for 15 min, and 293T cells were transfected using GeneChem transfection reagent (Shanghai GeneChem Co., Ltd.) according to the manufacturer's instructions. The transfected cells were incubated in serum-free medium for 6 h, the medium was subsequently replaced with medium containing 10% serum, and the cells were cultured for an additional 48-72 h. The packaging 293T cell line was transfected with the lentiviral vector.

The culture supernatants were collected when the cells expressed high levels of green fluorescence and cell fusion was observed (48-72 h). The virus in the supernatant was concentrated to the target volume by centrifugation (4˚C, 4,000 x g, 10 min). The viral concentrate was removed and aliquot into a tube for long-term storage at -80˚C. In order to determine the viral titer, 10 μl viral stock was used to make 1 ml serial dilutions (10^{-2}-10^{-6}), which were used to infect 293T cells in a 96-well plate ($4x10^4$ cells). Following 4 days in culture, EGFP expression in each well was observed under a fluorescence microscope (magnification, x200). The number of cells expressing EGFP was counted and multiplied by the dilution ratio to determine the viral titer [transducing units (TU)/ml]. The viral supernatant was harvested 48 h after transfection, and the lentiviral particle titer was determined ($5x10^8$ TU/ml).

The Tregs were cultured in 25 cm^2 culture flasks at a density of $1x10^6$ cells/ml. Following overnight culture, the cells were infected for 12 h at 37˚C with the lentiviral vector. Subsequently, the cells were washed and cultured in fresh medium for 3 days. The viral concentrates of shRNA-Helios were diluted to infect the UCB Tregs at a multiplicity of infection of 50. The transduction rate and expression of Helios in the Tregs were confirmed by flow cytometry (Fig. S1B and C).

Establishment of murine models of ALL. A total of 48 4-week-old female BALB/c nude mice (14±1 g) were obtained from Beijing HFK Bioscience (Beijing, China). The animals were housed in a specific pathogen-free environment, with

a constant temperature between 25˚C and 27˚C, in a 12/12 h light/dark cycle. The mice were fed with a standard diet and water *ad libitum*. On days 1 and 2, all mice received cyclophosphamide (2 mg/mouse; Heng Rui Medicine Co., Ltd., Jiangsu, China) by intraperitoneal injection. Animals in the blank group received PBS only on day 3. The model group was injected with Nalm-6 cells ($3x10^6$/mouse) through the tail vein on day 3. In the Helios^{low} group, Nalm-6 cells ($2.5x10^6$/mouse) were injected first through the tail vein on day 3, followed by UCB-derived Tregs ($0.6x10^6$/mouse) with shRNA-Helios transduction. In the Helios^{high} group, Nalm-6 cells ($2.5x10^6$/mouse) were injected first through the tail vein on day 3, followed by UCB-derived Tregs on day 14 of the culture period ($0.6x10^6$/mouse). Each group consisted of 12 mice. Mouse weights were determined once a week. In the Helios^{high} group, one mouse died on day 32 and another on day 41. In the model group, one mouse died on day 41. All mice were sacrificed on day 42 when the hind legs had become paralyzed in the majority of the leukemia model animals. The liver, spleen and kidneys were weighed to calculate the organ index, calculated as the organ weight to total body weight ratio. Bone marrow smears from the femur were examined in the Department of Pathology of Qilu Hospital. The use of the animals was approved by the Animal Care and Use Committee of Shandong University (Jinan, China).

Flow cytometry. The cells were stained with the following fluorochrome-conjugated antibodies: Phycoerythrin (PE) anti-human (h)CD19 (cat. no. SJ25C1, 12-0198, 0.06 μg/test; eBioscience; Thermo Fisher Scientific, Inc.), fluorescein isothiocyanate anti-hCD4 (cat. no OKT4, 11-0048, 0.25 μg/test; eBioscience; Thermo Fisher Scientific, Inc.), PE anti-hCD25 (cat. no BC96, 302606, 5 μl/test; BioLegend, Inc., San Diego, CA, USA), PerCP/Cy5.5 anti-mouse (m)CD4 (cat. no GK1.5, 100434, 0.25 μg/10^6 cells; BioLegend, Inc.), and allophycocyanin anti-mCD25 (cat. no 3C7, 101910, 0.25 μg/10^6 cells; BioLegend, Inc.). Allophycocyanin anti-human forkhead box P3 (hFoxP3; cat. no PCH101, 17-4776, 0.5 μg/test; eBioscience; Thermo Fisher Scientific, Inc.), PE anti-hHelios (cat. no 22F6, 12-9883, 0.03 μg/test; eBioscience; Thermo Fisher Scientific, Inc.) and Alexa Fluor® 488 anti-mFOXP3 (cat. no 150D, 320012, 5 μl/test; BioLegend, Inc.) were detected using the FoxP3/Transcription Factor Staining Buffer set (cat. no 00-5523; eBioscience; Thermo Fisher Scientific, Inc.) following the manufacturer's protocol. Analyses were performed using a Guava easyCyte 8HT flow cytometer (EMD Millipore), and the data were analyzed using Guava software 6.1. Multi-color flow cytometry with fluorescence minus one control was used to determine background signal levels.

Carboxyfluorescein diacetate succinimidyl ester (CFSE)-based proliferation and suppression assay. The proliferation capacity of the Treg population was detected as follows: Treg cells ($1x10^5$ cells/well) were labeled with 5 μM CFSE and incubated for 48 h at 37˚C in a 12-well plate. The proliferation of Treg cells was evaluated by flow cytometry.

The suppressive capacity of the Treg population was detected as follows: $CD4^+CD25^-$ Th cells were labeled with 5 μM CFSE and incubated for 48 h at 37˚C. The Tregs ($1x10^5$ cells/well) were cultured in RPMI-1640 medium supplemented with 100 U/ml rIL-2 and CD3/CD28 beads (bead: Cell ratio of 1:1; Invitrogen; Thermo Fisher Scientific, Inc.) at 37˚C. These Tregs were then co-cultured with Th cells for 72 h at 37˚C. The proliferation of Th cells was evaluated by flow cytometry. Modfit LT software (Version 3.1, Verity Software House, Inc., Topsham, ME, USA) was used for data analyses.

Western blotting. Western blotting was performed as described previously (9). Antibodies against VEGFA (cat. no. ab46154; 1:1,000; Abcam, Cambridge, MA, USA), VEGFR2 (cat. no. ab11939; 1:500; Abcam), VEGFR2 (phosphoS473; cat. no. ab5473; 1:800; Abcam), CD31 (cat. no. ab28364; 1:1,000; Abcam) and β-actin (cat. no. 60008-1-Ig; 1:2,000; ProteinTech Group, Inc.) were used. The proteins were detected using the ECL Chemiluminescence Detection kit (EMD Millipore) and quantitated with Image Studio Digits Ver 4.0 (LI-COR Biosciences, Lincoln, NE, USA). The signal intensities of all target proteins were normalized against β-actin signals.

In vitro vascular tube formation assay. To verify the effect of Helios$^+$ Tregs on endothelial tube formation, the culture supernatant of transfected Tregs was obtained by centrifugation at 800 x g for 10 minutes at room temperature. There were four groups: Blank group (blank), normal Tregs group on day 0 of the culture period (control), Tregs with high expression of Helios on day 14 of the culture period (Helios^{high} Treg), and Tregs with low expression of Helios (Helios^{low} Treg). Growth factor-reduced Matrigel (BD Biosciences, San Jose, CA, USA) was allowed to polymerize in a 96-well plate at 37˚C for at least 30 min. The HUVECs ($5x10^3$ cells /well) were suspended in 100 μl medium conditioned with culture supernatant from the normal Tregs (Control), Helios^{low} Tregs or Helios^{high} Tregs. Following incubation for 6 h at 37˚C, images of capillary-like structures in the Matrigel were captured under an Olympus IX71 inverted fluorescence microscope (Olympus Corporation, Tokyo, Japan). Tube formation was analyzed by determining the total tube length in each well using ImageJ software 1.43u (National Institutes of Health, Bethesda, MA, USA). The tube length of the entire culture well was measured. Fold changes of capillary length with respect to the control were determined. The total tube length of the blank group was set to one.

Immunohistochemical assessment of microvessel density (MVD). Paraffin-embedded and sliced bone marrow, liver and spleen tissues (4-μm thick) were produced by Servicebio Company (Wuhan, Hubei, China). The sections were prepared for microscopic examination by routine immunohistochemical methods using an antibody against CD31 (cat. no. ab28364, 1:50, Abcam). Low magnification (x100) was used to identify the regions of highest vascular density (hot spots), and three hot spots were selected to count the number of microvessels under high magnification (x400). A microvessel was considered as a brown-stained endothelial cell or endothelial cell cluster, with or without lumen, that was clearly separated from the adjacent tissue. The average value of these three counts represented the MVD for that case.

RNA isolation and reverse transcription-quantitative polymerase chain reaction (RT-qPCR) analysis. Total RNA was extracted from samples using TRIzol® reagent (Invitrogen;

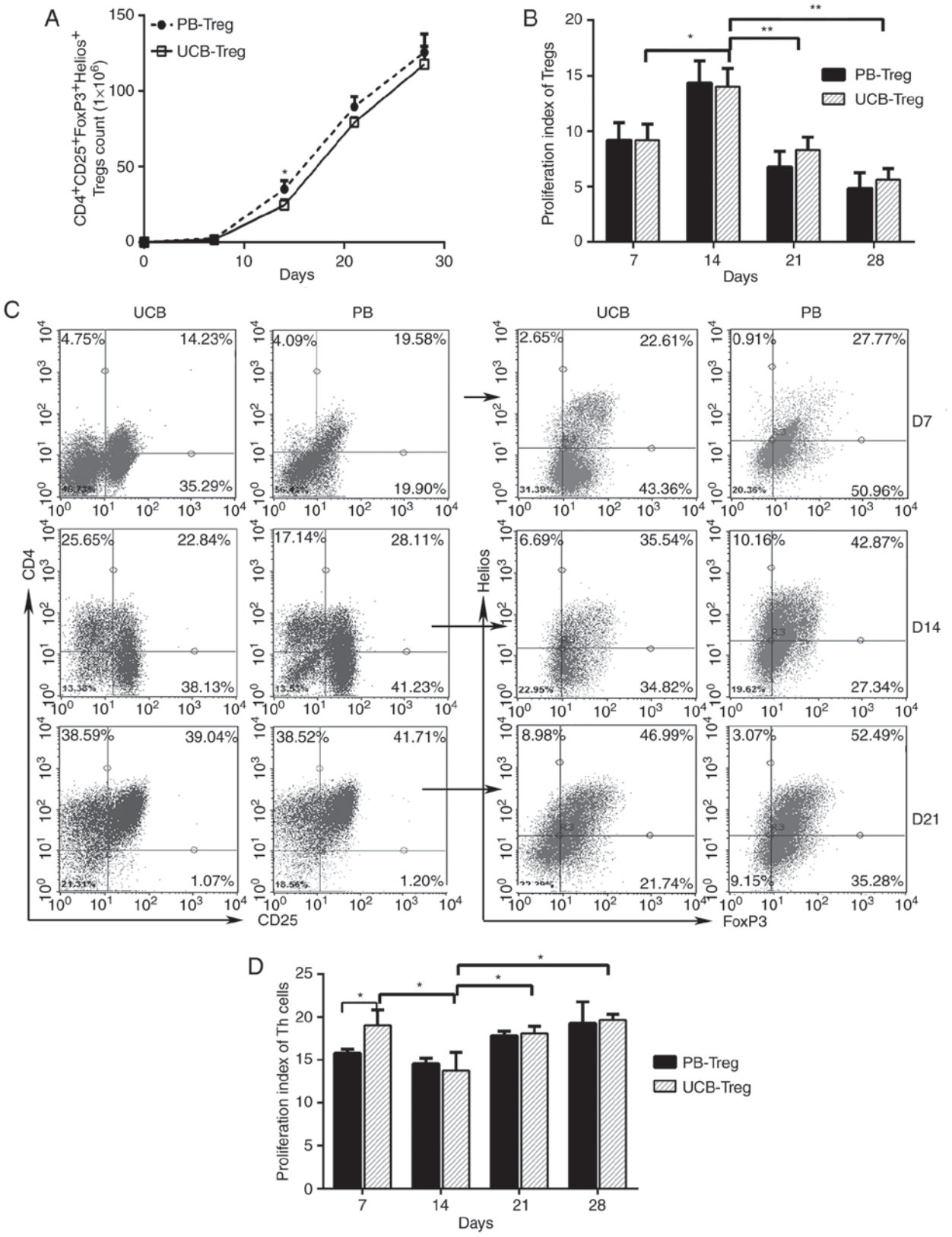

Figure 1. Number and suppressive function of Tregs isolated and expanded from UCB and PB. (A) Total numbers of $CD4^+CD25^+FoxP3^+Helios^+$ Tregs over time in the UCB and PB. (B) Proliferation indices of Tregs between days 7 and 28 in the UCB and PB, determined using a CFSE-based proliferation assay. (C) Proportions of $Helios^+FoxP3^+$ cells in $CD4^+CD25^+$ cell populations from UCB and PB determined by flow cytometry on days 7, 14 and 21. (D) Proliferation indices of Th cells in a CFSE-based suppression assay between days 7 and 28 of culture in UCB and PB. ($^{**}P<0.005$, $^{*}P<0.05$). UCB, umbilical cord blood; PB peripheral blood; CFSE, carboxyfluorescein diacetate succinimidyl ester; Treg, regulatory T cell; FoxP3, Forkhead box P3.

Thermo Fisher Scientific, Inc.). First-strand cDNA was synthesized using 1 μg of total RNA in a 20 μl of reverse transcription reaction mixture using the ReverTra Ace qPCR RT Master Mix kit (Toboyo Co., Ltd., Osaka, Japan) with primers. The

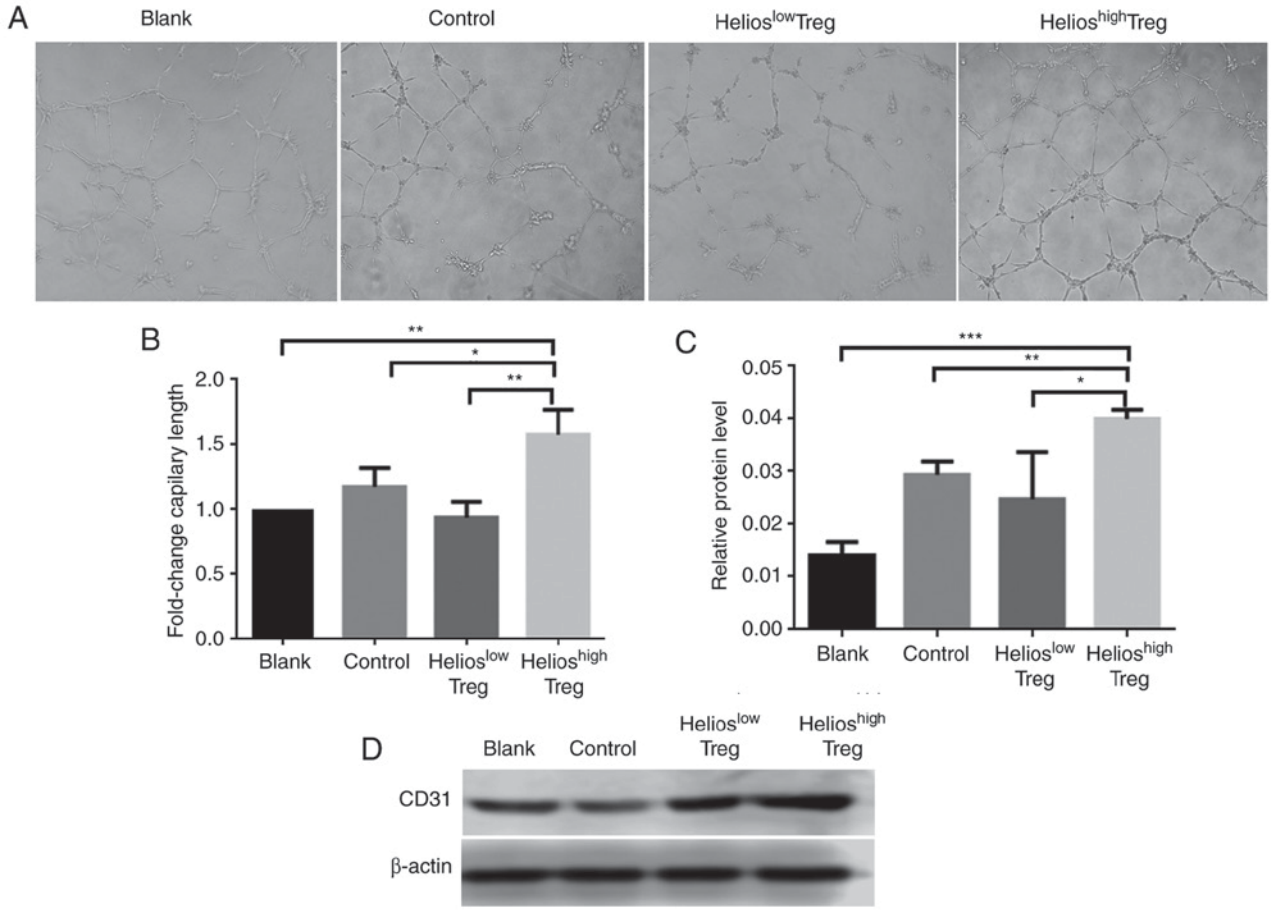

Figure 2. Helios enhances Treg-induced angiogenesis *in vitro*. (A) Micrographs of the tube formation assay using HUVECs incubated in supernatants from the blank, control, Helios^{low} Tregs and Helios^{high} Tregs groups (x200). (B) Quantitation of the tube formation assay. The total tube length of the blank group was set to one. (C) Western blot and (D) quantitative analyses of the protein expression of CD31 in human HUVECs incubated in supernatants from the blank, control, Helios^{low} Tregs and Helios^{high} Tregs groups. (***P<0.0005, **P<0.005, *P<0.05). Treg, regulatory T cell; HUVECs, human umbilical vein endothelial cells.

temperature protocol was as follows: 37˚C 15 min, 95˚C 5 min and 4˚C hold. qPCR analysis was performed on an ABI Prism 7500 sequence detection system using Thunderbird SYBR qPCR mix (Toboyo Co., Ltd.) in 20 μl of reaction mixture. The thermocycling conditions were as follows: Initial denaturation at 95˚C for 5 min, followed by 33 cycles of 95˚C (15 sec) and 60˚C (1 min). Data were analyzed using Sequence Detection Software 1.4 (Applied Biosystems; Thermo Fisher Scientific, Inc.). GAPDH was used as an internal control. Values for the blank group were set to one. RNA expression levels were quantified using the $2^{-\Delta\Delta Cq}$ method and normalized to the expression levels of GAPDH (12). The primer sequences are presented in Table SI.

Measurement of chemokine CC-chemokine ligand 22 (CCL22) by ELISA. Following the onset of ALL in mice, the mice were sacrificed and plasma was obtained by centrifugation at 1,000 x g for 10 minutes at room temperature for CCL22 protein detection. The protein levels of CCL22 were measured using an ELISA kit (cat. no. ab204525; Abcam) according to the manufacturer's protocol.

Statistical analysis. All data are presented as the mean ± standard deviation of three separate experiments. Differences in the number of PB-Tregs and UCB-Tregs, and the proportion of Helios^{+} cells following shRNA-Helios transduction were assessed using Student's t-test. Other experiments were assessed by one-way analysis of variance (ANOVA), which was used to compare multiple groups. If the ANOVA result was significant, the Bonferroni test was performed. Statistical analyses were performed using SPSS Statistics 17.0 (SPSS, Inc., Chicago, IL, USA). P<0.05 was considered to indicate a statistically significant difference.

Results

Isolation, amplification and identification of CD4^{+}CD25^{+}FoxP3^{+}Helios^{+} Tregs from fresh UCB. UCB is considered to be a universal source of Tregs, the function of which is not influenced by HLA antigen expression. The present study compared the proliferation and suppression abilities of CD4^{+}CD25^{+}FoxP3^{+}Helios^{+} Tregs derived from UCB and pediatric PB during the culture period. As shown in Fig. 1A, the number of induced CD4^{+}CD25^{+} Treg cells derived from the UCB and PB increased steadily between days 0 and 28. A statistically significant difference in the number of PB Treg cells and UCB Treg cells was observed on day 14. However, no significant differences in the numbers of these cells were observed on days 7, 21 and 28 of cultivation. On day 14, the proliferation capability of the Tregs

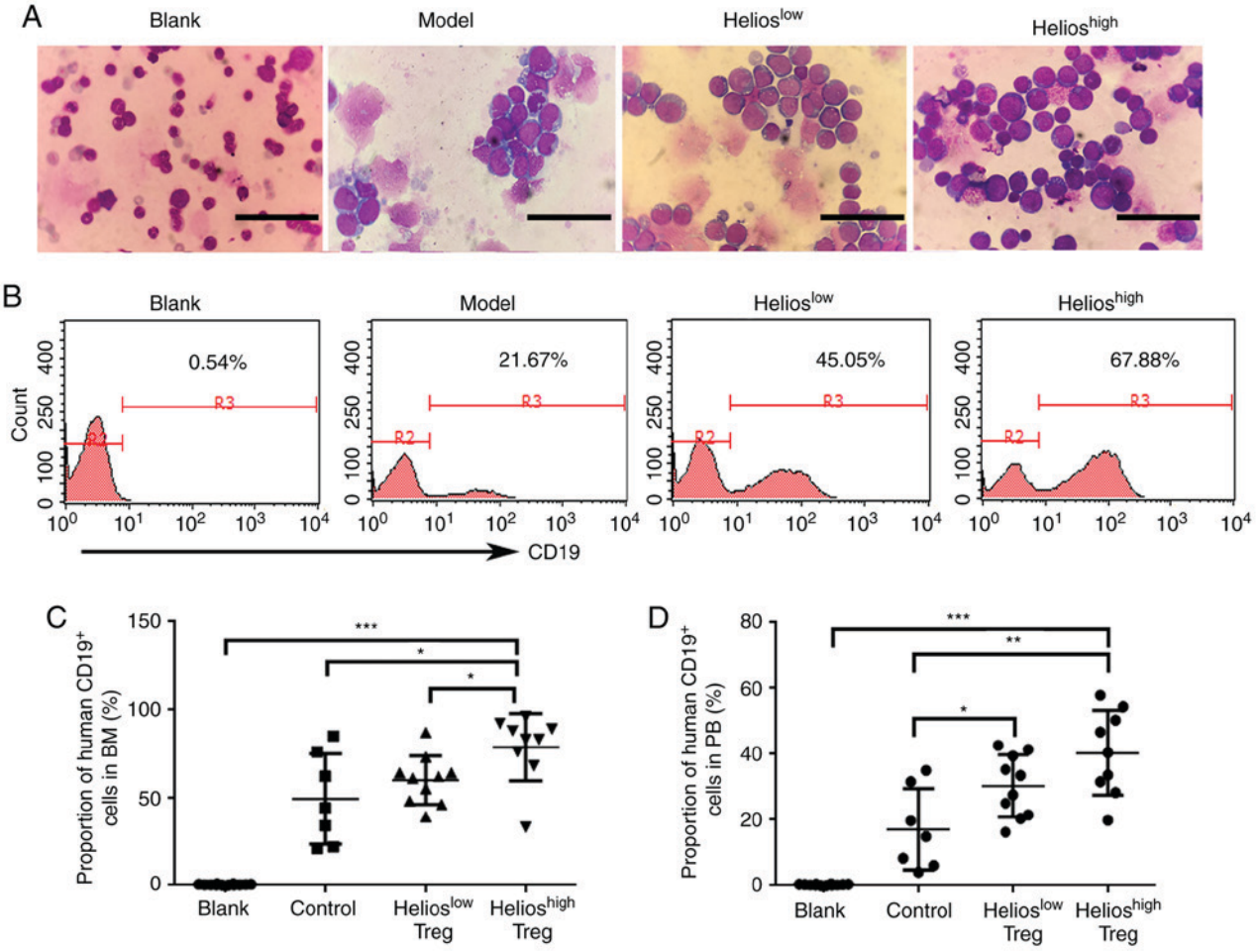

Figure 3. Helios$^+$ Tregs promote the infiltration of lymphoblasts in mouse models of acute lymphoblastic leukemia. (A) Proportions of lymphoblasts in the BM of the blank, model, Helios^{low} and Helios^{high} groups. Scale bar=25 μm. (B) Proportions and (C) quantitative analyses of human CD19$^+$ cells in the BM of the blank, model, Helios^{low} and Helios^{high} groups, determined by flow cytometry. (D) Quantitative analyses of human CD19$^+$ cells in the PB of the model, Helios^{low} and Helios^{high} groups. (***P<0.0005, **P<0.005, *P<0.05). BM, bone marrow; PB, peripheral blood; Treg, regulatory T cell.

was significantly enhanced in the UCB and PB (Fig. 1B). The ratio of Helios$^+$ FoxP3$^+$ T cells to isolated CD4$^+$CD25$^+$ T cells increased gradually between days 7 and 21, and reached a peak of almost 50% on day 21 (Fig. 1C). After day 21, cell debris significantly increased in the culture medium. The suppression ability of UCB Tregs was significantly enhanced on day 14 (Fig. 1D). On days 14, 21 and 28, the immunosuppressive ability of the UCB Treg cells did not differ significantly from that of the PB Treg cells (Fig. 1D). Based on the high expression of Helios and high immunosuppressive ability, Treg cells on day 14 of the culture period were selected for the subsequent experiments.

UCB-derived Helios$^+$ Tregs promote angiogenesis in vitro. The effect of Helios$^+$ Tregs on angiogenesis *in vitro* was subsequently examined. The results showed that, compared with the normal Tregs, the supernatant from Helios^{high} Tregs promoted angiogenesis (Fig. 2A and B). By contrast, inhibiting the expression of Helios in UCB Treg cells via shRNA-Helios reduced the angiogenic ability (Fig. 2A and B).

For further verification, protein levels of CD31 in HUVECs in the co-culture system were evaluated. Compared with the control and blank groups, the HUVECs incubated in supernatants from Helios^{high} Tregs exhibited higher protein levels of CD31. By contrast, when shRNA-Helios was present, the expression of CD31 was decreased (Fig. 2C and D).

UCB-derived Helios$^+$ Tregs increase the infiltration of leukemia cells into the bone marrow. The weights of mice with ALL were lower after 5 weeks compared with those in the blank group; however, there were no significant differences in weights among the three ALL groups (Fig. S2A). The ALL mice exhibited significant increases in the liver, spleen and kidney indices, compared with those in the normal nude mice. However, among the three ALL groups, no significant differences were observed in the liver, spleen or kidney indices (Fig. S2B). At 1 week post-Tregs infusion, neither human nor murine Tregs were detected in the PB of any groups.

Subsequently, the present study performed a BM smear to analyze the incidence of leukemia. Of the recipients, 90% (9/10) developed extensive bone marrow lymphoblastic infiltration in the Helios^{high} group. This was compared with 83% (10/12) in the Helios^{low} group, 64% (7/11) in the model group and 0% in the blank group (Fig. 3A). Furthermore, human CD19$^+$ cells in the BM were detected by flow cytometry. Compared with the model group and Helios^{low} group, the proportion of human CD19$^+$ cells in the BM was increased in the Helios^{high} group of ALL mice (Fig. 3B and C). Human CD19$^+$ cells were

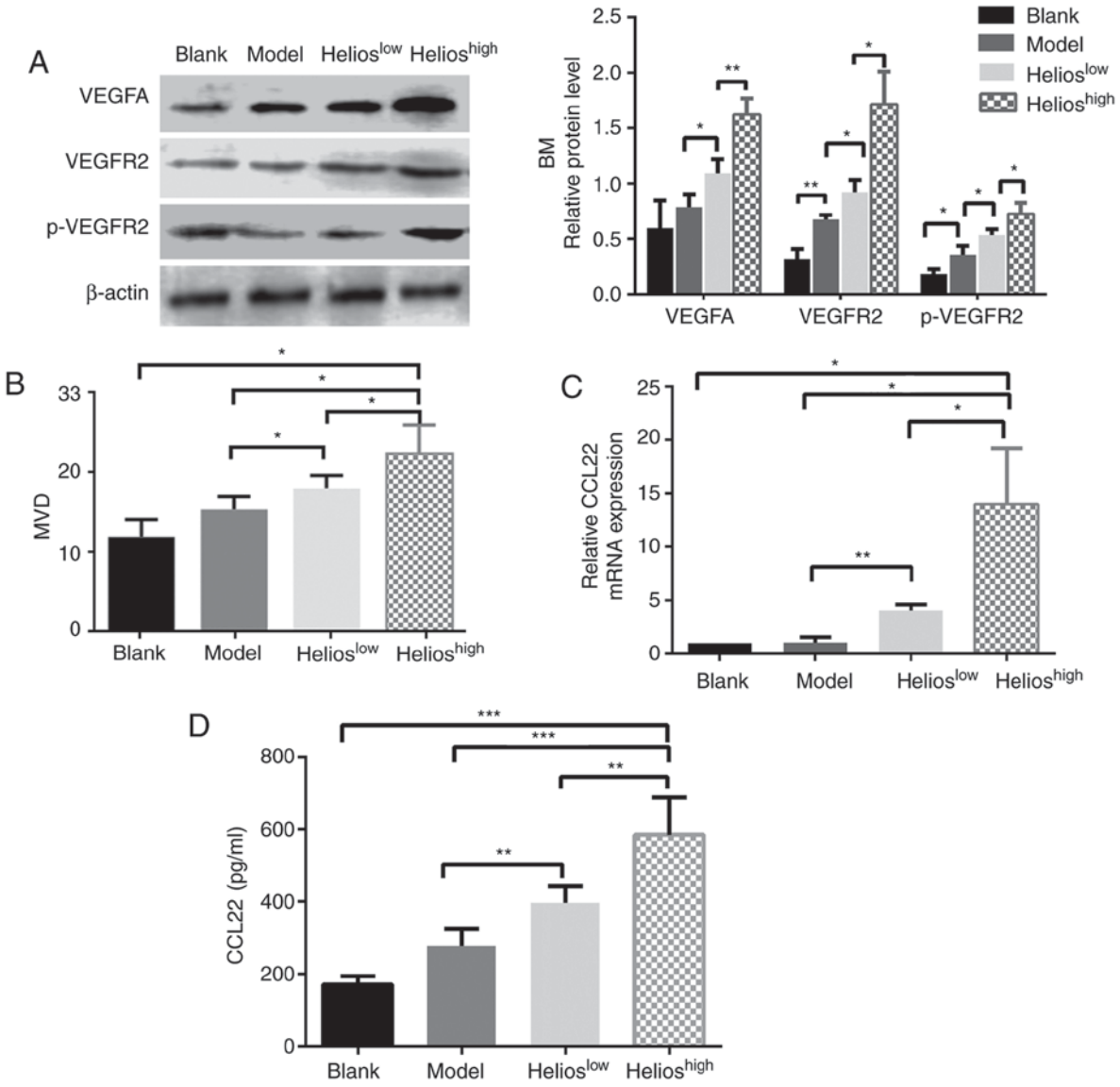

Figure 4. Helios$^+$ Tregs promote angiogenesis through the VEGFA/VEGFR2 pathway in a mouse model of acute lymphoblastic leukemia. (A) Western blot and quantitative analyses of VEGFA, VEGFR2 and p-VEGFR2 proteins in the BM of the blank, model, Helios^{high} and Helios^{low} groups. (B) Quantitative analyses of the CD31 MVD values of the BM in the blank, model, Helios^{low} and Helios^{high} groups. (C) Quantitation of the mRNA expression of CCL22 in the BM of the blank, model, Helios^{low} and Helios^{high} groups. (D) Quantitation of the protein levels of CCL22 in the plasma of the blank, model, Helios^{low} and Helios^{high} groups. (***P<0.0005, **P<0.005, *P<0.05). VEGF, vascular endothelial growth factor; VEGFR2, VEGF receptor 2; p-VEGFR2, phosphorylated VEGFR2; MVD, microvascular density; BM, bone marrow; CCL2, CC-chemokine ligand 22.

also detected in the PB. The accumulation of Tregs resulted in a higher number of transplanted primary leukemia cells, however, no differences were found between the Helios^{high} and Helios^{low} groups (Fig. 3D).

UCB-derived Helios$^+$ Tregs promote angiogenesis in ALL mice. The correlations between the accumulation of Helios$^+$ Tregs and biomarkers of angiogenesis, including VEGF family expression and MVD, were examined in four groups. In the bone marrow, the levels of VEGFA, VEGFR2 and phosphorylated (p)-VEGFR2 were increased in the mice infused with UCB-derived Tregs, and this was more marked in the Helios^{high} group (Fig. 4A). In the liver, spleen and kidneys of the ALL model mice, the protein expression levels of VEGFA, VEGFR1, VEGFR2 and p-VEGFR2 were significantly increased compared with those in the normal mice; however, no statistically significant differences in protein expression were observed among the three ALL groups (P>0.05).

The mean MVD was determined in the bone marrow, liver and spleen. The mice in the Helios^{high} group had higher MVD in the bone marrow (Fig. 4B), although no differences were present between the Helios^{high} and Helios^{low} groups with respect to the liver and spleen (P>0.05). The downstream genes regulated by Helios$^+$ Tregs were then identified. A higher expression of Helios in Tregs significantly increased the mRNA expression of CCL22 in the bone marrow (Fig. 4C), whereas the expression of other factors, including C-X-C motif chemokine ligand 6 (CXCL6), interleukin (IL)-17a, interferon-γ, TGF-β1, IL-10, CCL28 and neuropilin 1, remained unchanged (data not shown). Furthermore, the secretion of CCL22 protein in the plasma of mice was examined. The results showed that a higher expression of

Helios in Tregs significantly increased the protein expression of CCL22 in the plasma (Fig. 4D). When shRNA-Helios inhibited the expression of Helios in Tregs, the expression of CCL22 in the plasma decreased, compared with that in the Helios^{high} group (Fig. 4D).

Discussion

In the present study, an immunosuppressive internal environment was established by infusing a number of Helios$^+$CD4$^+$CD25$^+$FoxP3$^+$ Tregs into nude mice. The results confirmed that the infusion of Helios$^+$ Tregs increased the extent of leukemic cell infiltration in the bone marrow, with Helios serving a key role in angiogenesis. Consequently, Helios$^+$ Tregs are closely associated with the onset of leukemia, which is consistent with our previous study in pediatric patients with ALL (9).

Previous studies have reported a positive correlation between angiogenesis and tumor-infiltrating Tregs (13,14). Our previous study found an increase in the expression of Helios in ALL Tregs, and the capacity of PB-derived Helios$^+$ Tregs to ostensibly control the process of neovascularization *in vitro* (9). The present study confirmed that the overexpression of Helios in Tregs activated microvascular formation in the bone marrow of ALL mice. Due to the short onset time of ALL in mice, Treg cells may have mainly promoted leukemia cell infiltration of the bone marrow, which is the site of leukemia, and had minimal effect on liver and spleen infiltration. Therefore, the pro-angiogenic effect of Treg cells was mainly reflected in the bone marrow. Tregs can contribute to tumor angiogenesis through indirect and direct mechanisms. The mass of Tregs in the tumor microenvironment effectively restricts the Th 1 effect, which decreases the secretion of anti-angiogenic factors and indirectly promotes tumor angiogenesis (15). By contrast, Tregs can directly synthesize and secrete certain pro-angiogenic factors, including VEGF, neuropilin-l and apelin (16-18).

VEGF promotes tumor angiogenesis through stimulating the proliferation and survival of endothelial cells, and also by increasing the permeability of vessels and recruiting vascular precursor cells from the bone marrow (19). In the present study, the effects of Helios$^+$ Tregs on the microvasculature during ALL were mediated by the VEGFA/VEGFR2 pathway. VEGFA has been the subject of more investigations than other VEGF family members, and is a critical regulator of angiogenesis. VEGFR2 is the main signaling VEGFR in blood vascular endothelial cells (19,20). The blockade of VEGFA with a specific antibody decreases the number of Tregs, and inhibiting VEGFA/VEGFR-transduced signals counteracts the induction of Tregs by malignanT cells (21). Sunitinib, an agent targeting VEGFRs, has been reported to reduce the number of Tregs in tumor-bearing mice and in patients with metastatic renal carcinoma (22). Notably, the depletion of CD25$^+$ or CCR10$^+$ cells has been shown to eliminate Treg cells from the tumor microenvironment, and significantly suppress the expression of VEGF and angiogenesis at tumor sites (4). The present study demonstrated that the high expression of Helios in Tregs is an important factor in regulating bone marrow angiogenesis in ALL mice via the VEGF pathway.

Helios is expressed at relatively high levels in functional Tregs. Studies have shown that the overexpression of Helios enhances the immunosuppressive function of normal Tregs on Th cells (23). By contrast, Helios-deficient Tregs within tumors acquire effector T cell function and contribute to immune responses against cancer (11,24). CD4$^+$ invariant natural killer T cells protect from graft-versus-host disease-associated morbidity and mortality through an expansion of donor Helios$^+$ Tregs (25). Helios not only influences the expression of FoxP3, but also acts as a positive regulator of the TGF-β suppressor-effector function (9). A previous study found that tumor-infiltrating Tregs were mainly Helios$^+$ activated Tregs and significantly correlated with the concentration of CCL22 in ovarian tumor cell culture supernatants (26). The results of the present study also showed that a high expression of Helios in Tregs induced abnormal expression of the pro-angiogenic factor CCL22, which is responsible for Treg recruitment at tumor sites, and thus promoted angiogenesis further.

Chemokines have been shown to have pleiotropic effects in promoting tumor invasion, migration and vascularization (27). The upregulation of CCL28 caused by tumor hypoxia in ovarian cancer resulted in marked Treg accumulation, increased levels of VEGF and significantly increased blood vessel development (4). Tumor environments contain high levels of CCL22, which is likely derived from tumor cells and tumor macrophages (28). CCL22 can recruit Tregs through CCR4, and Treg migration can be abrogated through the inhibition of CCR4 *in vitro* (29). Human T-lymphotropic virus type 1 induces and maintains a high frequency of FoxP3$^+$ T cells by inducing expression of chemokine CCL22; the frequency is particularly high in patients with chronic leukemia (30). In the present study, a high expression of Helios in Treg cells stimulated macrophages, dendritic cells or leukemia cells to secrete CCL22, thereby recruiting Treg cells to the tumor site and then activating the VEGF signaling pathway to promote angiogenesis in tumor sites.

As a traditional and convenient source of cells for hematopoietic stem cell transplantation, UCB T cells contain a higher percentage of the naïve CD4$^+$CD25$^+$ subset compared with adult T cells (31). Therefore, the expansion of UCB Tregs can overcome the cell number limitation that often prevents their use (31,32). In the present study, UCB Helios$^+$ Tregs exhibited a similar proliferative capacity to pediatric PB Tregs. Although allogeneic Tregs from donors may offer improved therapeutic benefits, UCB Tregs have low immunogenicity and a high safety margin (33,34). Therefore, UCB may represent a safe and potent source for *in vitro* Treg expansion.

In conclusion, the results of the present study further clarify the mechanism of Tregs in the pathogenesis of ALL and highlight the impact of the Treg expression of Helios in on angiogenesis in ALL. These findings may assist in understanding the mechanisms by which Treg cells are involved in the pathogenesis of ALL, and may be useful for developing a molecular therapeutic strategy for ALL by targeting Tregs expressing Helios.

Acknowledgements

Not applicable.

Funding

This study was supported by Shandong Province Major Scientific Research Projects (grant nos. 2017GSF18155 and 2017GSF218015), the Shandong Province Natural Science Foundation (grant no. ZR2018MH012), the Ji'nan Science and Technology Development Foundation (grant no. 201704066) and the Shandong Province Natural Science Fund (grant no. 2014ZRE27630).

Availability of data and materials

The datasets used and/or analyzed during the current study are available from the corresponding author on reasonable request.

Authors' contributions

XJ and DL designed the study and drafted the manuscript; XL performed the cell culture and animal experiments, and was a major contributor in writing the manuscript. QS performed the *in vitro* vascular tube formation assay. XH performed CFSE-based proliferation and suppression assay. All authors read and approved the final manuscript.

Ethics approval and consent to participate

All study participants, including direct participants, blood donors and parent/guardians of child participants provided written informed consent. The study was approved by the Research Ethics Committee of Qilu Hospital and the use of the animals was approved by the Animal Care and Use Committee of Shandong University.

Patient consent for publication

Not applicable.

Competing interests

The authors declare that they have no competing interests.

References

1. Nishikawa H and Sakaguchi S: Regulatory T cells in tumor immunity. Int J Cancer 127: 759-767, 2010.
2. Takeuchi Y and Nishikawa H: Roles of regulatory T cells in cancer immunity. Int Immunol 28: 401-409, 2016.
3. Duell J, Dittrich M, Bedke T, Mueller T, Eisele F, Rosenwald A, Rasche L, Hartmann E, Dandekar T, Einsele H and Topp MS: Frequency of regulatory T cells determines the outcome of the T-cell-engaging antibody blinatumomab in patients with B-precursor ALL. Leukemia 31: 2181-2190, 2017.
4. Facciabene A, Peng X, Hagemann IS, Balint K, Barchetti A, Wang LP, Gimotty PA, Gilks CB, Lal P, Zhang L and Coukos G: Tumour hypoxia promotes tolerance and angiogenesis via CCL28 and T(reg) cells. Nature 475: 226-230, 2011.
5. Weis SM and Cheresh DA: Tumor angiogenesis: Molecular pathways and therapeutic targets. Nat Med 17: 1359-1370, 2011.
6. Facciabene A, Motz GT and Coukos G: T-regulatory cells: key players in tumor immune escape and angiogenesis. Cancer Res 72: 2162-2171, 2012.
7. Yang J, Yan J and Liu B: Targeting VEGF/VEGFR to modulate antitumor immunity. Front Immunol 9: 978, 2018.
8. Aguayo A, Kantarjian H, Manshouri T, Gidel C, Estey E, Thomas D, Koller C, Estrov Z, O'Brien S, Keating M, *et al*: Angiogenesis in acute and chronic leukemias and myelodysplastic syndromes. Blood 96: 2240-2245, 2000.
9. Li X, Li D, Huang X, Zhou P, Shi Q, Zhang B and Ju X: Helios expression in regulatory T cells promotes immunosuppression, angiogenesis and the growth of leukemia cells in pediatric acute lymphoblastic leukemia. Leukemia Res 67: 60-66, 2018.
10. Getnet D, Grosso JF, Goldberg MV, Harris TJ, Yen HR, Bruno TC, Durham NM, Hipkiss EL, Pyle KJ, Wada S, *et al*: A role for the transcription factor Helios in human CD4(+)CD25(+) regulatory T cells. Mol Immunol 47: 1595-1600, 2010.
11. Kim HJ, Barnitz RA, Kreslavsky T, Brown FD, Moffett H, Lemieux ME, Kaygusuz Y, Meissner T, Holderried TA, Chan S, *et al*: Stable inhibitory activity of regulatory T cells requires the transcription factor Helios. Science 350: 334-339, 2015.
12. Livak KJ and Schmittgen TD: Analysis of relative gene expression data using real-time quantitative PCR and the 2(-Delta Delta C(T)) method. Methods 25: 402-408, 2001.
13. D'Alessio FR, Zhong Q, Jenkins J, Moldobaeva A and Wagner EM: Lung angiogenesis requires CD4(+) forkhead homeobox protein-3(+) regulatory T cells. Am J Respir Cell Mol Biol 52: 603-610, 2015.
14. Woidacki K, Meyer N, Schumacher A, Goldschmidt A, Maurer M and Zenclussen AC: Transfer of regulatory T cells into abortion-prone mice promotes the expansion of uterine masT cells and normalizes early pregnancy angiogenesis. Sci Rep 5: 13938, 2015.
15. Miyara M, Ito Y and Sakaguchi S: TREG-cell therapies for autoimmune rheumatic diseases. Nat Rev Rheumatol 10: 543-551, 2014.
16. Terme M, Pernot S, Marcheteau E, Sandoval F, Benhamouda N, Colussi O, Dubreuil O, Carpentier AF, Tartour E and Taieb J: VEGFA-VEGFR pathway blockade inhibits tumor-induced regulatory T-cell proliferation in colorectal cancer. Cancer Res 73: 539-549, 2013.
17. Yadav M, Louvet C, Davini D, Gardner JM, Martinez-Llordella M, Bailey-Bucktrout S, Anthony BA, Sverdrup FM, Head R, Kuster DJ, *et al*: Neuropilin-1 distinguishes natural and inducible regulatory T cells among regulatory T cell subsets *in vivo*. J Exp Med 209: 1713-1722, S1711-1719, 2012.
18. Leung OM, Li J, Li X, Chan VW, Yang KY, Ku M, Ji L, Sun H, Waldmann H, Tian XY, *et al*: Regulatory T cells promote apelin-Mediated sprouting angiogenesis in Type 2 diabetes. Cell Rep 24: 1610-1626, 2018.
19. Sia D, Alsinet C, Newell P and Villanueva A: VEGF signaling in cancer treatment. Curr Pharm Des 20: 2834-2842, 2014.
20. Shibuya M: VEGF-VEGFR signals in health and disease. Biomol Ther(Seoul) 22: 1-9, 2014.
21. Terme M, Tartour E and Taieb J: VEGFA/VEGFR2-targeted therapies prevent the VEGFA-induced proliferation of regulatory T cells in cancer. Oncoimmunology 2: e25156, 2013.
22. Xin H, Zhang C, Herrmann A, Du Y, Figlin R and Yu H: Sunitinib inhibition of Stat3 induces renal cell carcinoma tumor cell apoptosis and reduces immunosuppressive cells. Cancer Res 69: 2506-2513, 2009.
23. Syed Khaja AS, Toor SM, El Salhat H, Ali BR and Elkord E: Intratumoral foxP3(+)helios(+) regulatory T cells upregulating immunosuppressive molecules are expanded in human colorectal cancer. Front Immunol 8: 619, 2017.
24. Nakagawa H, Sido JM, Reyes EE, Kiers V, Cantor H and Kim HJ: Instability of Helios-deficient Tregs is associated with conversion to a T-effector phenotype and enhanced antitumor immunity. Proc Natl Acad Sci U S A 113: 6248-6253, 2016.
25. Schneidawind D, Pierini A, Alvarez M, Pan Y, Baker J, Buechele C, Luong RH, Meyer EH and Negrin RS: CD4+ invariant natural killer T cells protect from murine GVHD lethality through expansion of donor CD4+CD25+FoxP3+ regulatory T cells. Blood 124: 3320-3328, 2014.
26. Fialova A, Partlova S, Sojka L, Hromádková H, Brtnický T, Fučíková J, Kocián P, Rob L, Bartůňková J and Spíšek R: Dynamics of T-cell infiltration during the course of ovarian cancer: The gradual shift from a Th17 effector cell response to a predominant infiltration by regulatory T-cells. Int J Cancer 132: 1070-1079, 2013.
27. Kumai T, Nagato T, Kobayashi H, Komabayashi Y, Ueda S, Kishibe K, Ohkuri T, Takahara M, Celis E and Harabuchi Y: CCL17 and CCL22/CCR4 signaling is a strong candidate for novel targeted therapy against nasal natural killer/T-cell lymphoma. Cancer Immunol Immunother 64: 697-705, 2015.

28. Niens M, Visser L, Nolte IM, van der Steege G, Diepstra A, Cordano P, Jarrett RF Te Meerman GJ, Poppema S and van den Berg A: Serum chemokine levels in Hodgkin lymphoma patients: Highly increased levels of CCL17 and CCL22. Br J Haematol 140: 527-536, 2008.
29. Pere H, Montier Y, Bayry J, Quintin-Colonna F, Merillon N, Dransart E, Badoual C, Gey A, Ravel P, Marcheteau E, *et al*: A CCR4 antagonist combined with vaccines induces antigen-specific CD8+ T cells and tumor immunity against self antigens. Blood 118: 4853-4862, 2011.
30. Bangham CR and Toulza F: Adult T cell leukemia/lymphoma: FoxP3(+) cells and the cell-mediated immune response to HTLV-1. Adv Cancer Res 111: 163-182, 2011.
31. Brunstein CG, Miller JS, McKenna DH, Hippen KL, DeFor TE, Sumstad D, Curtsinger J, Verneris MR, MacMillan ML, Levine BL, *et al*: Umbilical cord blood-derived T regulatory cells to prevent GVHD: Kinetics, toxicity profile, and clinical effect. Blood 127: 1044-1051, 2016.
32. Seay HR, Putnam AL, Cserny J, Posgai AL, Rosenau EH, Wingard JR, Girard KF, Kraus M, Lares AP, Brown HL, *et al*: Expansion of human tregs from cryopreserved umbilical cord blood for GMP-compliant autologous adoptive cell transfer therapy. Mol Ther Methods Clin Dev 4: 178-191, 2017.
33. Theil A, Tuve S, Oelschlagel U, Maiwald A, Döhler D, Oßmann D, Zenkel A, Wilhelm C, Middeke JM, Shayegi N, *et al*: Adoptive transfer of allogeneic regulatory T cells into patients with chronic graft-versus-host disease. Cytotherapy 17: 473-486, 2015.
34. Brunstein CG, Miller JS, Cao Q, McKenna DH, Hippen KL, Curtsinger J, Defor T, Levine BL, June CH, Rubinstein P, *et al*: Infusion of *ex vivo* expanded T regulatory cells in adults transplanted with umbilical cord blood: Safety profile and detection kinetics. Blood 117: 1061-1070, 2011.